

Finite-amplitude double-component convection due to different boundary conditions for two compensating horizontal gradients

N. Tsitverblit*

Department of Fluid Mechanics and Heat Transfer, Tel-Aviv University, Ramat-Aviv 69978, Israel

(Received 10 December 1999; revised manuscript received 5 July 2000)

Finite-amplitude convective steady flows that do not bifurcate from the respective conduction state are discovered. They arise as the compensating horizontal gradients of two density-affecting components with equal diffusivities but different boundary conditions are applied to the Boussinesq fluid at rest with and without stable vertical stratification. These flows emanate from convection in a laterally heated stably stratified slot. Their relevance to convective states in a horizontal slot with two vertical gradients, emphasizing universality of the underlying type of convection, is discussed.

PACS number(s): 47.20.Bp, 47.15.Fe, 47.15.Rq, 47.20.Ky

Applications of double-component convection range from oceanography [1,2] and astrophysics [3,4] to crystal growth [5] and colloidal suspensions [6]. Convective flows are also commonly used to study transition to turbulence and nonlinear pattern formation [7,8]. Up until recently, two-component convection in pure fluid had been mainly associated only with the effect of different diffusion coefficients [9–11]. Generalizing the idea of Welander [12], it has recently been suggested in [13–15] that there is a fundamental physical analogy between the effect of different boundary conditions and that of different diffusivities. The component whose values are fixed at the boundaries would have a higher perturbation gradient than the one with the flux boundary conditions. The differential diffusion resulting from this disparity could thus be expected to trigger convection analogously to the classical double-diffusion. In particular, this was demonstrated in [15] for a laterally heated stably stratified slot (LHSSS) [16].

The primary convection pattern, whose formation is a prerequisite of the transition to turbulence in the system, is usually expected to emanate from the respective linear instability of the conduction base flow. This seems to have not applied only to binary-fluid convection [17], if the separation ratio is negative. The present work reports the manifestation of pure-fluid convection in the form of finite-amplitude steady flows that do not bifurcate from the conduction state of a layer of Boussinesq fluid. These flows arise from the effect of different boundary conditions as such conditions maintain two compensating horizontal gradients of the components with equal diffusivities in the fluid at rest (with and without stable vertical stratification). These solutions are shown to be a continuation of the convective states in a LHSSS. They are also expected to result from continuous transformation of the convective flows in a horizontal slot in [13,14]. All convective steady states arising from the effect of boundary conditions in diverse configurations [13–15] could thus be described by the single formulation.

Let the diffusivities of the components be equal and the compensating horizontal gradients be maintained by differ-

ent boundary conditions at vertical no-slip walls. The diffusivities are set equal to extract the effect of boundary conditions, or they could be viewed as eddy coefficients. Both gradients are represented by the Rayleigh number $Ra = g\alpha|\Delta\bar{T}|d^3/\kappa\nu = g\beta|\partial\bar{S}/\partial\bar{x}|d^4/\kappa\nu$. Here, \bar{x} is the (dimensional) horizontal coordinate, d is the width of the vertical slot, $\Delta\bar{T}$ is the (dimensional) difference between the values of temperature (the fixed-value component, or the component diffusing faster) at the sidewalls, $\partial\bar{S}/\partial\bar{x}$ is the sidewalls-prescribed (dimensional) horizontal derivative of solute concentration (the flux component, or the component diffusing slower), α is the coefficient of thermal expansion, β is the coefficient of the density variation due to the variation of solute concentration, g is the gravitational acceleration, ν is the kinematic viscosity, and $\kappa = \kappa_T = \kappa_S$ is the diffusivity of both components. The bar means that the respective variable is dimensional.

Using the same numerical approach as in [15], the two-dimensional problem just described was examined for the Boussinesq fluid by continuation of the background no-flow solution in Ra . Despite the analogy it has with the classical double-diffusive configuration in [18], however, no indication of the Jacobian sign change being possible was found up to $Ra \sim 2 \times 10^6$, at least for any vertical wavelength $\lambda = \bar{\lambda}/d \leq 6$. Such finding was also independently confirmed by direct examination of the eigenvalues of the 8×8 matrix of the boundary conditions imposed on the general solution of the steady, marginal linear stability problem. NAG Fortran routines were used.

Let a stable vertical solute stratification, characterized by the Rayleigh number $Ra_S = g\beta|\partial\bar{S}/\partial\bar{y}|d^4/\kappa\nu$ (\bar{y} is the vertical coordinate), be also present. This problem (Fig. 1, $\varphi = 0$) is addressed herein. At first sight, its background state is nearly identical to that in the LHSSS in [15], where an opposing horizontal solute gradient arises due to vertical motion. However, the Jacobian in the above range of λ and Ra showed no trend towards its sign change even for Ra_S at which double-component instability arises in a LHSSS ($\sim 30\,000$, for example [15]).

Let $\varphi = 0$ (Fig. 1) and let a cut of such slot in Fig. 1 be with the vertically periodic conditions, $\lambda = 2$, and Ra_S being

*Address for correspondence: 1 Yanosh Korchak Street, Apt. 6, Netanya 42495, Israel. Email address: naftali@eng.tau.ac.il

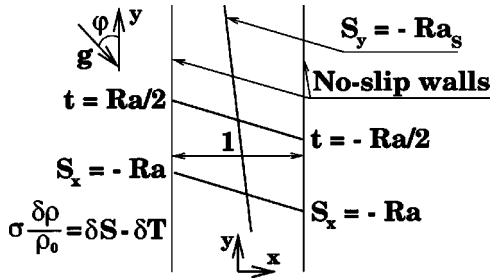


FIG. 1. The problem in a vertical ($\varphi=0$) and inclined ($\varphi>0$) slot. $\delta\rho=\rho-\rho_0$ is the variation of the (nondimensional) density, ρ , due to the variations δS and δT of solute concentration S and temperature $T=(T_1+T_2)/2+t$ with respect to their reference values, at which the density is ρ_0 ; T_1 and T_2 are the sidewall temperatures, $\sigma=g d^3/\kappa\nu$. $\text{Pr}=\nu/\kappa=6.7$, $\kappa_S=\kappa_T=\kappa$; κ_T and κ_S are the component diffusivities. The fluid is of the Boussinesq type.

in the region of double-component instability of a LHSSS (say $\sim 30\,000$). For the sidewall boundary conditions, however, let us introduce a more general formulation ($S=-\text{Ra}_S y+s$):

$$\omega = \frac{\partial^2 \psi}{\partial x^2}, \quad \psi=0, \quad t = \pm \frac{\text{Ra}}{2},$$

$$\frac{\partial s}{\partial x} = -\mu \text{Ra} \quad (x=0,1, \quad 0 \leq y \leq \lambda). \quad (1)$$

Here ω is the vorticity and ψ is the streamfunction. For $\mu=1$, (1) gives the present problem (Fig. 1, $\varphi=0$). At $\mu=0$, however, boundary conditions (1) identifies a LHSSS. A nearly compensating horizontal solute gradient is then formed (outside the sidewall boundary layers) by the vertical flow [16]. One can thus verify if a convective state bifurcating from such flow at $\mu=0$ persists at $\mu=1$, where the background horizontal solute gradient is due to the sidewall flux. Such problem is described by boundary conditions (1) along with the Eqs. (1)–(4) and periodic conditions (9) in [15].

The basic result of this work is that, as $\text{Le}=\kappa_T/\kappa_S=1$, the convective states arising at $\mu=0$ and large enough Ra_S (say $\geq 10^4$) were successfully continued in μ to $\mu=1$. As seen from Fig. 2, the steady linear stability margin goes to infinity when μ increases from $\mu=0$ to $\mu \geq \sim 0.8$. The finite-amplitude stability boundary, however, barely changes, thus exhibiting a purely nonlinear manifestation of convection. For $\mu>0.5$, changes of the Jacobian sign were detected along the unstable branch A1, indicating that additional solutions exist. These bifurcations do not restore stability of any part of branch A1, and thus were not addressed in this work. For this reason, they are not presented in Fig. 2. The scenario for $\mu=1$ in Fig. 2 is reminiscent of the one proposed in [19]. Such scenario also seems to arise in binary-fluid convection [17].

The convective states at $\mu=1$ are illustrated in Fig. 3. As $\text{Ra}_S=0$ or small, such flows are reached by continuation in Ra_S from a large enough Ra_S , where they are obtained by continuation in μ from $\mu=0$. As seen from Fig. 3, the lateral temperature gradient in the vicinity of a sidewall towards which the horizontal component of motion is directed is higher than the gradient of solute concentration. Caused by the different sidewall boundary conditions, this effect produces a horizontal density difference between two streamline

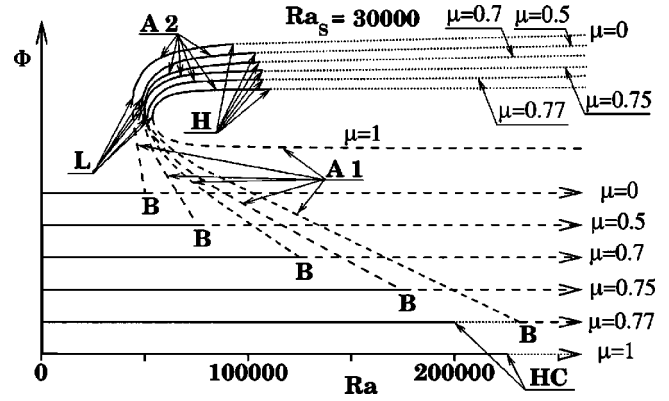


FIG. 2. $\varphi=0$. Schematic structures of steady flows for $\mu \in [0,1]$; $\text{Ra}_S=30\,000$ ($\text{Pr}=6.7$, $\text{Le}=1$), $\lambda=2$. The background states are depicted by the horizontal lines with arrows (for $\mu=1$, this is the coordinate axis). The solid lines stand for the stable solutions. The dashed lines stand for the flows being unstable to either steady or both steady and oscillatory disturbances. The dotted lines stand for the solutions being unstable to oscillatory disturbances alone. B is the subcritical bifurcation standing for the steady linear stability boundary; it moves to infinite Ra as $\mu \rightarrow \mu_c \approx 0.8$. Φ is an abstract measure of the symmetric component of the steady flows. L is the limit point standing for the finite-amplitude stability boundary. The variation of its Ra , Ra_L , is overemphasized: for $\mu \in [0,1]$, Ra_L monotonically increases within interval [45 652, 52 894]. A1 and A2 are the unstable and stable (to steady disturbances) branches associated with the limit point, respectively. HC and H are Hopf bifurcations (Table I). At the unstable flows, Hopf bifurcations were not sought.

points. This maintains the cellular motion. When $\text{Ra}_S>0$, the vertical scale of such a motion is additionally limited. Such cell height is proportional to $\eta=\alpha|\Delta T|/(\beta|\partial \bar{S}/\partial \bar{y}|)=\text{Ra}/\text{Ra}_S d$ [Figs. 3(a) and 3(d)], as suggested in [20]. It also remains of the order of η if the period allows [Fig. 3(b)].

Another finding is oscillatory instability of the conduction state and branch A2, associated with respective Hopf bifurcations (Table I). Hopf bifurcation HC in Fig. 2 seems to emanate from the directly unstable region of the background flow at $\mu \leq 0.75$ [where linear time evolution of the (growing) perturbation also exhibited oscillatory behavior], intersecting steady bifurcation B at $\mu \in (0.75, 0.77)$. HC at $\mu=1$ and $\text{Ra}_S=0$ suggests the possibility of an oscillatory manifestation of the effect of boundary conditions in such problems. The present numerical formulation is only reflectionally symmetric, as the periodic conditions (9) in [15] fix the flow phase. With the translation symmetry of the conduction state being also allowed for, such Hopf bifurcation as HC could give rise to two oscillatory branches [21]. This possibility and its implications will be addressed separately.

Let an infinite slot with two opposing across-slot gradients and the along-slot orientation of the gravity be such that the linear double-component steady instability arises in it. This could be a LHSSS, for example. The convective steady state could not then be symmetric with respect to the sense of rotation of its cells. The cells whose sense of rotation creates locally unstable along-slot solute perturbation stratification would dominate those where such stratification is stable. Such bifurcation, if any, is thus prone to be subcritical [15,16,18], due to the disparity between the stable finite-

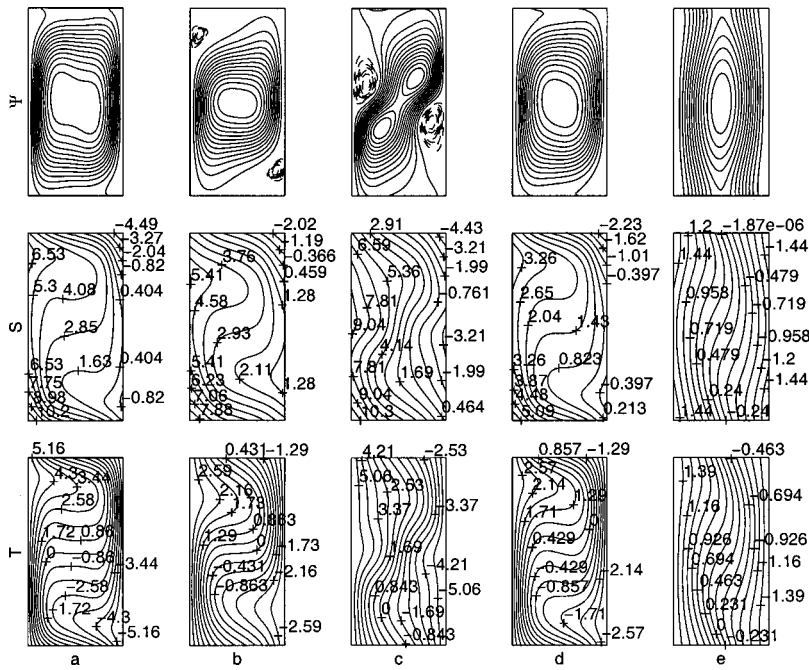


FIG. 3. $\varphi=0$. Convective steady flows at $\mu = 1$ ($Pr=6.7$, $Le=1$); $\lambda=2$. Ψ : streamlines; S : isolines of (full) solute concentration; T : isotherms [t in (1)]. The solid ($\psi>0$) and dashed ($\psi<0$) streamlines are equally spaced within $(0, \psi_{\max})$ and $(\psi_{\min}, 0)$ and represent the clockwise and counterclockwise rotation, respectively; $\psi_{\min}=\inf(\psi)$, $\psi_{\max}=\sup(\psi)$. The actual values of t and S are equal to 10^4 times the ones in the figure. (a) $Ra_S=30\,000$, $Ra=120\,394$, branch A2, $\psi_{\max}=1842$, $\psi_{\min}=0$; (b) $Ra_S=30\,000$, $Ra=60\,394$, branch A2, $\psi_{\max}=1084$, $\psi_{\min}=-10$; (c) $Ra_S=30\,000$, $Ra=117\,981$, branch A1 (directly unstable), $\psi_{\max}=550$, $\psi_{\min}=-93$; (d) $Ra_S=15\,000$, $Ra=60\,000$, branch A2, $\psi_{\max}=1531$, $\psi_{\min}=0$; (e) $Ra_S=0$, $Ra=32\,394$, branch A2 (unstable to oscillatory disturbances at this Ra), $\psi_{\max}=1230$, $\psi_{\min}=0$.

amplitude pattern and symmetric counter-rotating cells initially forming at the onset of linear instability. (In particular, the unstable branch of the subcritical bifurcation thus permits steady transition between these two patterns.) In other words, finite-amplitude steady instability is more generic for such systems: its existence is a necessary condition for the respective linear instability.

The key element of the steady instability mechanism described in [14] is feedback between the vertical displacement of a fluid particle and disparity in the perturbed vertical diffusion gradients. Such feedback exists due to the different boundary conditions. Parallel to the gravity, the across-slot component of perturbed motion is thus directly maintained

by the (gradient) differential diffusion even as the initial perturbation is infinitesimal.

In the present configuration, however, the across-slot direction is perpendicular to the gravity. The feedback energy for further horizontal advance of a perturbed fluid particle could come from the perturbation vorticity generated by the cell-forming differential (lateral gradient) diffusion. This involves along-slot dissipation. The along-slot component of perturbed motion is damped by dissipation in the geometry of [14] as well. In that geometry, however, this component is not part of the feedback between the across-slot displacement and disparity in the perturbation gradients. Such feedback in a system with two opposing horizontal gradients, therefore,

TABLE I. $\varphi=0$. Onset of oscillatory instability of the conduction state (HC) and branch A2 (H) and the values of Ra of limit point L , Ra_L , as functions of Ra_S ; $\mu=1$, $\lambda=2$. Ra_{st} and Ra_{un} are the maximal stable and minimal unstable values of Ra , respectively, at which the stability of the flows was examined; f_{st} and f_{un} are the respective frequencies (inverse periods) of the most unstable mode, nondimensionalized with ν/d^2 (the inverse time scale). The frequencies were calculated from the power spectrum densities of the linear evolutions resulting from the initial perturbation proportional to the whole steady solution vector (with 1024 time steps $\delta\tau=0.05$ for HC and $\delta\tau=0.1$ for H).

		$Ra_S/1000$ ($Pr=6.7$, $Le=1$)						
		0	5	10	15	20	25	30
Ra_{st}	HC	17	46	79	113	151	191	223
	H	8.5	31	50	68	86	104	121
Ra_{un}	HC	18	47	80	114	152	192	224
	H	9	32	51	69	87	105	122
f_{st}	HC	0.64	1.02	1.27	1.46	1.64	1.80	2.19
	H	0.30	0.75	0.90	0.99	1.05	1.11	1.15
f_{un}	HC	0.64	1.04	1.29	1.48	1.66	1.80	2.19
	H	0.32	0.77	0.91	0.99	1.05	1.11	1.16
Ra_L		6427	17 603	26 147	33 628	40 462	46 847	52 894

is not as efficient as in [14]. Thus a small-amplitude steady perturbation is generally less likely to develop this type of feedback in such a system than in the geometry of [14].

At $\mu=0$, the specific conditions for development of the infinitesimal steady perturbation are apparently more favorable than in the present problem. In particular, the vanishing background horizontal solute gradient near the sidewalls at $\mu=0$ reduces the across-slot scale of this component compared to that at $\mu=1$. Since this scale specifies the relative solute perturbation amplitude at the onset, such adjustment of parameters could prove to be critical for development of the infinitesimal perturbation. Indeed, let the relative solute perturbation amplitude in Fig. 2(a) of [15] increase. Analogous to the effect of enhancement of the background across-slot solute scale with growing μ , this tends to decrease the horizontal density-perturbation contrast at a perturbation streamline. At sufficiently large μ , such contrast would thus fail to maintain the illustrated type of infinitesimal perturbation.

Let us consider an inclined slot in Fig. 1 ($\varphi>0$) and let $Ra_S=0$. For $\varphi=\pi/2$, this is just a particular case of the problem in [14] with no-slip boundaries. As mentioned above, the convective mechanism in the latter configuration causes linear steady instability, whereas the instability is of the finite-amplitude nature in the present problem. As φ changes from $\pi/2$ to 0, the projection of the gravity on the (x) axis perpendicular to the plates, responsible for the linear instability mechanism discussed in [14], decreases. At the same time, the emerging along-slot (y) component of the gravity is enhanced. As already discussed, the latter component introduces asymmetry between the senses of rotation of the counter-rotating convection cells.

With φ changing from $\pi/2$ to 0, therefore, the convective steady pattern of reflectionally symmetric counter-rotating cells in the horizontal slot would have to transform into the one where the clockwise-rotating cells are dominant. As suggested above, this growing cell asymmetry should eventually render the instability subcritical. With the across-slot (x) component of the gravity further decreasing as φ approaches 0 (the present problem), it would also be natural that the linear steady instability (caused by this component) vanish.

The present convective flows (Fig. 3) could thus correspond just to different values of φ and Ra_S of convective states bifurcating supercritically from the no-flow solution in the no-slip version of the slot in [13,14]. (They could therefore be relevant to the ocean Langmuir circulations arising in the presence of stable vertical stratification [2], for the no-slip boundary conditions are transformable by continuation into the stress-free ones in [2].) Trial computations, where φ was the continuation parameter and $Ra_S=0$, indicated that this should indeed be the case. The detailed analysis of the corresponding transformations will be reported separately.

Exhibiting an essentially nonlinear onset of pure-fluid convection, the discovered flows could thus also permit continuous transformation (with varying μ , Ra_S , and φ , in particular) between any two convective steady states arising from the effect of boundary conditions in diverse configurations. This emphasizes the universal nature of the convection resulting from the disparity between diffusion gradients in perturbed state of a double-component fluid system with different boundary conditions.

-
- [1] R. W. Schmitt, *Annu. Rev. Fluid Mech.* **26**, 255 (1994).
 [2] S. Leibovich, *Annu. Rev. Fluid Mech.* **15**, 391 (1983).
 [3] E. A. Spiegel, *Annu. Rev. Astron. Astrophys.* **10**, 261 (1972).
 [4] D. W. Hughes and M. R. E. Proctor, *Annu. Rev. Fluid Mech.* **20**, 187 (1988).
 [5] S. R. Coriell and R. F. Sekerka, *PCH, PhysicoChem. Hydrodyn.* **2**, 281 (1981).
 [6] D. M. Mueth, J. C. Crocker, S. E. Esipov, and D. G. Grier, *Phys. Rev. Lett.* **77**, 578 (1996).
 [7] R. P. Behringer, *Rev. Mod. Phys.* **57**, 657 (1985).
 [8] M. C. Cross and P. C. Hohenberg, *Rev. Mod. Phys.* **65**, 851 (1993).
 [9] M. E. Stern, *Tellus* **12**, 172 (1960).
 [10] G. Veronis, *J. Mar. Res.* **23**, 1 (1965).
 [11] M. E. Stern, *Deep-Sea Res.* **14**, 747 (1967).
 [12] P. Welander, *Tellus, Ser. A* **41**, 66 (1989).
 [13] N. Tsitverblit, in *Double-Diffusive Processes*, edited by S. Meacham, Woods Hole Oceanographic Institution, Technical Report No. WHOI-97-10, 1997, pp. 145–159.
 [14] N. Tsitverblit, *Phys. Fluids* **9**, 2458 (1997).
 [15] N. Tsitverblit, *Phys. Fluids* **11**, 2516 (1999).
 [16] S. A. Thorpe, P. K. Hutt, and R. Soulsby, *J. Fluid Mech.* **38**, 375 (1969); J. E. Hart, *ibid.* **49**, 279 (1971); **59**, 47 (1973); S. Thangam, A. Zebib, and C. F. Chen, *ibid.* **112**, 151 (1981); Y. Young and R. Rosner, *Phys. Rev. E* **57**, 5554 (1998); O. S. Kerr and K. Y. Tang, *J. Fluid Mech.* **392**, 213 (1999).
 [17] W. Barten, M. Lücke, M. Kamps, and R. Schmitz, *Phys. Rev. E* **51**, 5636 (1995); see also the references therein.
 [18] S. Xin, P. Le Quééré, and L. S. Tuckerman, *Phys. Fluids* **10**, 850 (1998) and references therein.
 [19] S. Rosenblat and S. H. Davis, *SIAM (Soc. Ind. Appl. Math.) J. Appl. Math.* **37**, 1 (1979).
 [20] C. F. Chen, D. G. Briggs, and R. A. Wirtz, *Int. J. Heat Mass Transf.* **14**, 57 (1971).
 [21] J. D. Crawford and E. Knobloch, *Annu. Rev. Fluid Mech.* **23**, 341 (1991).